doi:10.1246/cl.2010.870
Published on the web July 10, 2010

Speciation of Tungsten in Natural Ferromanganese Oxides Using Wavelength Dispersive XAFS

Teruhiko Kashiwabara,*[1] Yoshio Takahashi,[1] Tomoya Uruga,[2] Hajime Tanida,[2]
Yasuko Terada,[2] Yasuhiro Niwa,[3] and Masaharu Nomura[3]
[1]*Department of Earth and Planetary Systems Science, Hiroshima University, Hiroshima 739-8526*
[2]*SPring-8, Japan Synchrotron Radiation Research Institute (JASRI), Sayo-cho, Sayo-gun, Hyogo 679-5198*
[3]*Photon Factory, Institute of Materials Structure Science, KEK, Oho, Tsukuba, Ibaraki 305-0801*

(Received May 13, 2010; CL-100464; E-mail: teruhiko-hekeke@hiroshima-u.ac.jp)

Reliable speciation of tungsten (W) in natural ferromanganese oxides was realized by wavelength-dispersive XAFS using a Laue-type analyzer. The quality of W L_3-XANES spectrum was greatly enhanced by this method compared to that measured by conventional fluorescence mode, and it was found that W in natural ferromanganese oxides was in octahedral symmetry.

Elemental distribution at solid/water interface is an important process in many fields of geochemistry. In marine environments, distribution between seawater and ferromanganese oxides (FMO), which is prevalent aggregates of iron hydroxides and manganese oxides, has great impact on concentrations of trace elements in seawater.[1,2] For example, molybdenum (Mo) in marine environments is controlled by this process, since ca. 70% of output is presumed to be incorporated into FMO in the budget of Mo in the marine system.[3] In addition, large isotopic fractionation of Mo occurs during adsorption on FMO, leading to the heavier isotope of Mo remaining in seawater.[3] Isotopic composition of Mo in seawater is also affected by the reaction of Mo at solid/water interface.

In this manuscript, the main topic is the speciation of tungsten (W) in natural FMO. Although W and Mo are congeners, they show contrasting distribution behaviors under different redox conditions.[4] In the oxic seawater, enrichment factor of W into FMO is two orders of magnitude greater than that of Mo,[5] the cause of which is still unknown. Some previous studies suggested the importance of the molecular structure for distribution of various elements at solid/water interface.[6,7] For Mo, local structure in natural FMO was already revealed by our previous XAFS analysis.[8] However, XAFS analysis of W has not yet been achieved because of some analytical problems, leading to lack of structural information of W in the natural samples which may be critical for the enrichment mechanism.

In this study, we applied wavelength-dispersive XAFS and obtained structural information of W in natural FMO for the first time. This method previously enabled us to improve the quality of XAFS spectra of some trace elements in environmental samples.[9,10] For trace elements, fluorescence XAFS is conventionally conducted with an energy-dispersive detector, such as a Ge solid-state detector (Ge-SSD). However, this detector has an upper counting limit in the order of 10^5 (photons/s), which originates from pulse-shaping time of the amplifier at 100 ns order. Thus, intense scattering and fluorescence from predominant elements such as Fe and Mn and/or interferences of K lines of Ni, Cu, and Zn (1000 mg kg^{-1}–2%) inhibit us from obtaining high quality fluorescence XAFS spectra of W (< 100 mg kg^{-1}). To deal with this problem, we introduced bent crystal Laue analyzer (BCLA) in front of the Ge-SSD, which enabled selective extraction the L line of W and to obtain the spectra with high S/B and S/N ratios.

As a natural sample, hydrogenetic ferromanganese nodule (AD14) was obtained from the Pacific Ocean (14.1°N, 167°W, 1617 m depth).[11] The powdered sample was packed into a polyethylene bag for XAFS analysis. Average major element compositions were (Mn, Fe) = (29.5 wt %, 16.7 wt %), while concentrations of coexisting elements which can interfere with the L line of W were (Ni, Cu, Zn) = (3450 mg kg^{-1}, 904 mg kg^{-1}, 1420 mg kg^{-1}).[11,12] In this sample, W content was 49.1 mg kg^{-1}, measured by ICP-MS. In the measurement of W L_3-edge XAFS by fluorescence mode, the interferences of Ni Kβ (8.265 keV), Cu Kβ (8.402 keV), and Zn Kα (8.632 keV) lines cause serious problems for the detection of the W Lα line (8.398 keV). For the W Lβ line (9.846 keV), on the other hand, the Zn Kβ line (9.572 keV) and scattering of incident X-ray overlap. Thus, we compared fluorescence XANES spectra measured using Lα and Lβ lines with BCLA to find the best analytical condition.

XAFS measurements were conducted at BL37XU in SPring-8 (Hyogo, Japan). The X-rays from undulator were monochromatized by a Si(111) double-crystal monochromator. Two horizontal mirrors were used for harmonic rejection. Beam size was adjusted to 200(V) μm × 300(H) μm at the sample by slits. All the spectra were collected in the fluorescence mode using a 19-element Ge solid-state detector, in front of which BCLA (DCA-0950, Oxford Danfysik) was placed. These measurements were conducted under ambient conditions. More experimental details can be found in previous related studies.[9,10]

Tungsten L_3-edge XANES spectra are shown in Figure 1 (before background subtraction) and Figure 2 (A: normalized after background subtraction, B: their second derivatives). In conventional measurement by detection of the Lα line (Figures 1(a), 2A(a), and 2B(a)), the raw spectrum (Figure 1(a)) showed high background noise levels mainly due to the intense interference of Ni, Cu, and Zn, which leads to poor quality of the spectra (a) in Figures 2A and 2B. In contrast, efficient removal of the background was found by introduction of BCLA (Figure 1(c)), leading to a clearer shape in the spectra (c) in Figures 2A and 2B. To evaluate the spectral quality, S/B and S/N ratios were defined as the ratio of the signal intensity at 10.200 keV (S) to the background intensity before absorption edge (B) and as the ratio of S to standard deviation 3σ of absorption data from 10.100 to 10.150 keV (N), respectively. As a result, 13-fold improvement in the S/B ratio and 4.8-fold improvement in the S/N ratio were achieved by the application of BCLA; those without BCLA were 0.11 and 6.6 (Figure 1(a)), whereas those with BCLA were 1.5 and 32 (Figure 1(c)), respectively. In addition, we also examined the detection of the

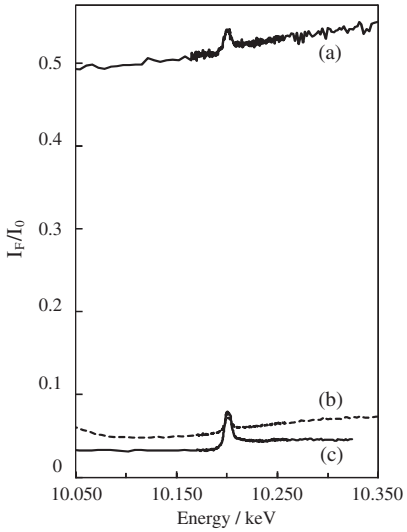

Figure 1. Tungsten L_3-edge XANES spectra of natural ferromanganese oxides before background subtraction measured by detection of (a) Lα line without BCLA, (b) Lβ line with BCLA, and (c) Lα line with BCLA.

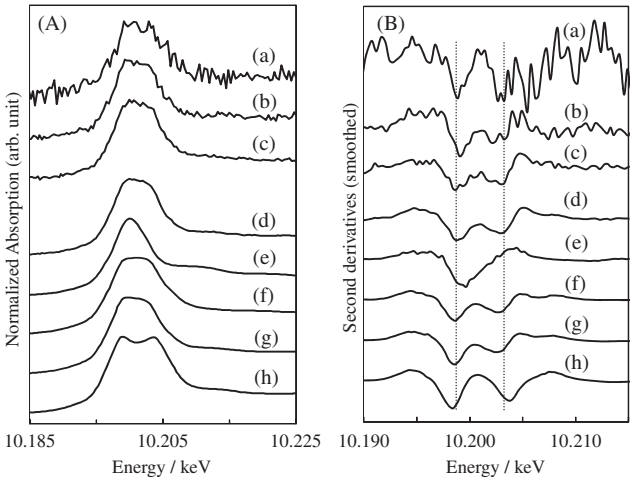

Figure 2. Tungsten L_3-edge XANES spectra after background subtraction. (A) Normalized spectra and (B) their second deviations. (a)–(d): AD14 measured by detection of (a) Lα line without BCLA, (b) Lβ line with BCLA, (c) Lα line with BCLA, and (d) Lα line with BCLA (sum of 7 spectra). (e) $Na_2WO_4 \cdot 2H_2O$, (f) WO_3, (g) $(NH_4)_{10}W_{12}O_{41}$, and (h) Cr_2WO_6.

Lβ line with BCLA (Figures 1(b), 2A(b), and 2B(b)). Indeed, S/B and S/N ratios in Figure 1(b) were improved from conventional mode (Figure 1(a)) but worse than the detection of the Lα with BCLA (Figure 1(c)). A curved spectrum in pre- and post-edge regions for the spectrum (b) in Figure 1 can be caused by the contaminant of the scattering of incident X-ray close to the Lβ line, which may be a problem for the XAFS measurement. Therefore, we concluded that the Lα detection with BCLA is the best method for the W L_3-edge XAFS measurement of natural FMO containing 49.1 mg kg^{-1} of W with 1000–3500 mg kg^{-1} of Ni, Cu, and Zn.

The prominent peak in W L_3-edge XANES is caused by the 2p $\rightarrow$ 5d transition. The splitting in their second derivatives depends on the degree of the symmetry of W, which corresponds to ligand field splitting of d orbitals.[13] Each reference compound in Figure 2B shows a different energy gap between two peaks corresponding to the symmetry of W: $Na_2WO_4 \cdot 2H_2O$ ((e), T_d symmetry), WO_3 ((f), distorted O_h symmetry), $(NH_4)_{10}W_{12}O_{41} \cdot 5H_2O$ ((g), distorted O_h symmetry), and Cr_2WO_6 ((h), D_2 symmetry). On the other hand, the spectrum of natural sample with BCLA (Figure 2B(d)), summation of 7 scans, clearly showed the degree of splitting equal to Figures 2B(f) and 2B(g). Thus, we concluded that W in the natural FMO is in distorted octahedral symmetry. Although, it is known that the dominant species of W in seawater is tetrahedral WO_4^{2-},[14] this is the first structural data of W in FMO, directly revealed by wavelength-dispersive XAFS method.

EXAFS analysis is needed to discuss the difference of distribution mechanisms of W and Mo, which is related to their solubilities into seawater or enrichment into natural FMO. On the other hand, the finding in this study can be important for isotope geochemistry. In the case of Mo, large isotopic fractionation occurs during adsorption on manganese oxides which originates from the structural difference between dissolved and adsorbed species.[8] In contrast, Mo shows little or no fractionation during adsorption on iron hydroxides due to the similarity of local structure between adsorbed and dissolved species.[8] These isotopic behaviors of Mo can be used to study paleocean redox conditions.[8] For W, isotopic fractionation is also expected based on the molecular symmetry revealed in this study, although isotopic study of W in FMO has not been reported yet. Future isotopic data are needed to show the relationship between the structure and isotopic fractionation.

We thank Y.S. Shimamoto for her contribution to this work. This work has been performed with the approvals of JASRI (Nos. 2009A1668, 2009B1383, 2009B1720, and 2010A1407)

References

1 R. Chester, *Marine Chemistry*, Cambridge Univ. Press, **1990**, Vol. 382, p. 6137.
2 Y. Takahashi, A. Manceau, N. Geoffroy, M. A. Marcus, A. Usui, *Geochim. Cosmochim. Acta* **2007**, *71*, 984.
3 C. Siebert, T. F. Nägler, F. von Blanckenburg, J. D. Kramers, *Earth Planet. Sci. Lett.* **2003**, *211*, 159.
4 Y. Sohrin, M. Matsui, E. Nakayama, *Geochim. Cosmochim. Acta* **1999**, *63*, 3457.
5 N. Takematsu, Y. Saito, S. Okabe, A. Usui, *Mar. Chem.* **1990**, *31*, 271.
6 T. Harada, Y. Takahashi, *Geochim. Cosmochim. Acta* **2008**, *72*, 1281.
7 A. Manceau, L. Charlet, *J. Colloid Interface Sci.* **1994**, *168*, 87.
8 T. Kashiwabara, Y. Takahashi, M. Tanimizu, *Geochem. J.* **2009**, *43*, e31.
9 Y. Takahashi, T. Uruga, H. Tanida, Y. Terada, S. Nakai, H. Shimizu, *Anal. Chim. Acta* **2006**, *558*, 332.
10 Y. Yamamoto, Y. Takahashi, Y. Kanai, Y. Watanabe, T. Uruga, H. Tanida, Y. Terada, H. Shimizu, *Appl. Geochem.* **2008**, *23*, 2452.
11 T. Kashiwabara, S. Mitsunobu, A. Das, T. Itai, M. Tanimizu, Y. Takahashi, *Chem. Lett.* **2008**, *37*, 756.
12 Y. Takahashi, H. Shimizu, A. Usui, H. Kagi, M. Nomura, *Geochim. Cosmochim. Acta* **2000**, *64*, 2929.
13 S. Yamazoe, Y. Hitomi, T. Shishido, T. Tanaka, *J. Phys. Chem. C* **2008**, *112*, 6869.
14 F. J. Millero, *Chemical Oceanography*, 3rd ed., CRC Press, **2006**, p. 91.

